

Photoluminescence of amorphous silicon at low temperatures: Computer simulation

E. I. Levin, S. Marianer, and B. I. Shklovskii

Theoretical Physics Institute, University of Minnesota, 116 Church St. SE, Minneapolis, Minnesota 55455

(Received 24 May 1991; revised manuscript received 21 November 1991)

Recombination and photoluminescence in amorphous silicon are studied using a computer simulation. It is shown that, in typical experimental situations, geminate recombination plays a minor role and most of the recombination events are distant-pair ones. The shapes and the positions of the luminescence peaks of time-resolved spectroscopy (TRS) and frequency-resolved spectroscopy (FRS) are studied and an approximate analytic theory to calculate them is derived. The width of the peaks obtained in our simulation is approximately two decades in time in the whole range of generation rates. These results are in good agreement with the experimental data as well as with our analytic theory. The possibility to observe a second, geminate, TRS and FRS peak in amorphous materials with strong polaron effects is discussed.

I. INTRODUCTION

The observation of unexpectedly high photoconductivity (PC) in hydrogenated amorphous silicon (a -Si:H) near liquid-helium temperatures^{1,2} and of the lifetime distributions of the photoluminescence (PL) (Refs. 3 and 4) have stimulated renewed interest in the motion and fate of carriers in the tail states. PL studies have already established that PL is the dominant recombination mechanism at low temperatures and that nonradiative processes can be neglected. There is, however, no commonly accepted point of view about the relative roles of geminate and distant-pair (nongeminate) radiative recombinations in undoped a -Si:H. Street⁵ suggested that geminate recombination dominates, but Dunstan and Boulitrop⁶ and recently Searle⁷ gave convincing arguments for distant-pair recombination. It is well known that only nongeminately recombining carriers contribute to PC,¹ therefore the competition between the two types of recombination plays a most important role for PC. It is also important for the calculation of the steady-state concentration of carriers, the distribution of PL times, and for PL spectra.

To discuss this competition let us consider a typical electron-hole pair created by light absorption.⁸ If the carriers are created with energies close to the mobility edges, they become trapped in the band tails and separate by diffusion due to downward hopping. In the course of separation the radiative recombination with the geminate carrier competes with diffusion that tears the pair apart. If the diffusion is fast enough that a typical pair can survive geminate recombination, its carriers can easily meet carriers from other pairs and distant-pair recombination will dominate. On the other hand, if the diffusion is slow or the interpair distance is large, the pair will likely recombine geminately. Shklovskii, Fritzsche, and Baranovskii⁸ analyzed the fate of an isolated electron-hole pair created on neighboring localized states and introduced the function $P(R)$, which gives the probability density of geminate recombination at a separation R .

This function has a maximum at some distance R_c and a long tail at $R > R_c$ (see Fig. 1). Using this function the steady-state concentration of electrons n and the photoconductivity σ_{PC} were estimated.^{8,9} Shklovskii, Fritzsche, and Baranovskii⁸ suggested that due to the exponential dependence of the recombination time on the distance R , the function $P(R)$ can give the probability density of the lifetime distribution observed by time-resolved spectroscopy (TRS) (Ref. 5) or frequency-resolved spectroscopy (FRS).¹⁰ In this paper we use the term TRS for the so-called biased TRS technique, which obtains the distribution of the logarithms of lifetimes from the decay of the light intensity after a small pulse excitation on the background of steady illumination.¹⁰ In the FRS technique similar information is extracted from the measurement of luminescence under harmonically modulated illumination. Strictly speaking, there is a minor difference between the results of these two methods and we discuss this difference in Appendix A.

The suggestion by Shklovskii, Fritzsche, and Baranovskii⁸ is of course valid only in the limit of very small concentrations n (or small generation rates G) when

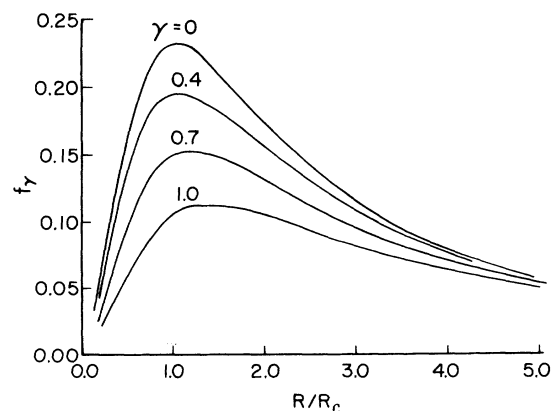


FIG. 1. The dimensionless geminate distribution densities $f_\gamma(R/R_c) \equiv R_c P_\gamma(R)$ for several values of the parameter $\gamma = a_n/a_e$.

the distance at which nongeminate recombination takes place $\frac{1}{2}n^{-1/3}$ is much larger than R_c . In *a*-Si:H we obtain that $R_c \lesssim \frac{1}{2}n^{-1/3} \lesssim 2R_c$ in the experimentally studied range of generation rates $10^{17} < G < 10^{22} \text{ cm}^{-3} \text{ s}^{-1}$. Searle⁷ and Levin *et al.*¹¹ presented arguments, based on the shape of $P(R)$, that in this range distant-pair recombination dominates and determines the shape of the FRS peak.

In this paper we present a direct Monte Carlo simulation of low-temperature recombination and PL in amorphous semiconductors under a constant illumination as well as an approximate analytical theory of the TRS and FRS peaks.

In the simulation we study a cube with 5×10^5 randomly spaced localized states with energies randomly distributed according to the exponential density of states in the tails of the conduction and valence bands. We create electrons and holes randomly on close pairs of states with a given generation rate G and let them relax by downward hopping and recombine with each other. We obtain the concentration of carriers n and TRS and FRS spectra as functions of G . We find that in the experimental range of generation rates only a small fraction of the carriers (less than 20%) recombine geminately, in agreement with Dunstan and Boulitrop.⁶ The widths of the spectra are much smaller than those obtained from the geminate theory and the function $P(R)$. These widths do not depend on G and are about a factor 100 in lifetime. This result agrees both with our analytical theory and with the experimental data. The maximum of the peak coincides with the average lifetime and varies as G^{-5} , where $s \approx 0.84$.

Thus we conclude that in typical experimental conditions in *a*-Si:H downward hopping easily separates electron-hole pairs. To verify this conclusion we repeated the simulation creating electrons and holes in random states rather than in close ones. We found very small differences in the TRS and FRS spectra and concentrations. If one assumes that when the carriers are created in the extended states they thermalize fast enough and reach the localized states, it becomes clear why the PL and PC of *a*-Si:H do not change significantly when the frequency of illumination changes from $h\nu < E_g$ to $h\nu > E_g$,¹² where E_g is the mobility gap.

The results discussed above were obtained for parameters of *a*-Si:H, where the characteristic frequency of the phonon-assisted hopping is much larger than that of the radiative recombination. In some softer materials with a strong polaron effect diffusion can be much less effective and geminate recombination will play a more important role. In these materials we expect different FRS structures depending on the relation between $h\nu$ and E_g . For $h\nu < E_g$ two peaks should be observed, one related with $P(R)$ and the other related with distant-pair recombination, while for $h\nu > E_g$ one should see only the distant-pair peak.

The paper is organized as follows. In Sec. II we summarize the theory of geminate recombination and derive an approximate analytic theory for distant-pair recombination. In Sec. III we describe our computer simulation and the information that can be obtained from it.

Section IV is devoted to a detailed description of the simulation results and to a comparison of these results with experiment. Finally, we give a brief summary and conclusions in Sec. V.

II. BASIC THEORETICAL CONCEPTS

In this section we summarize some theoretical results^{8,9} and present additional ones along the same line. Let us consider an electron-hole pair generated at or just below the mobility edge of an amorphous semiconductor. The pair is generated quite close together because of the exponential decay of the overlap integral with the distance. First we discuss the fate of one electron-hole pair assuming for simplicity that the hole is fixed in space. The electron can take part in two competing processes. First it can hop downward in energy (upward hops are not possible at $T=0$) to a nearest localized state of the tail at a distance r with the rate

$$v_d(r) = v_0 \exp\left[-\frac{2r}{a_e}\right], \quad (1)$$

where a_e is the localization radius of the electron. It was shown^{8,9} that, since the electron chooses the nearest accessible state, the concentration of accessible states decreases in a geometrical progression with the number of hops and, therefore, the length r increases geometrically starting from $r_0 \sim a_e$. The second process is recombination with the hole at a rate

$$v_r(R) = \tau_0^{-1} \exp\left[-\frac{2R}{a_e}\right], \quad (2)$$

where R is the electron-hole separation. We assume for a while that the localization radius of the hole $a_h \ll a_e$ and we can neglect the motion of the hole.

One should note the different prefactors of Eqs. (1) and (2). The prefactor $v_0 \approx 10^{12} \text{ s}^{-1}$, whereas $\tau_0^{-1} \approx 10^8 \text{ s}^{-1}$ is given by the typical dipole radiation lifetime τ_0 . These prefactors define a characteristic length scale

$$R_c = (a_e/2) \ln(v_0 \tau_0). \quad (3)$$

It is clear from Eqs. (1) and (2) that due to the strong inequality $v_0 \tau_0 = 10^4 \gg 1$ diffusion dominates for the first steps and a real competition between recombination and hopping starts only when R reaches a value of about R_c . A pair survival probability $\eta(R)$ to a distance R and a geminate recombination probability density $P(R) = -d\eta/dR$ were introduced in Refs. 8 and 9 and it was found that

$$P(R) = \frac{1}{R_c} f_0(R/R_c). \quad (4)$$

The function $P(R)$ is shown in Fig. 1 and has the shape described in the Introduction. Its magnitude is small when $R < R_c$ because diffusion dominates at these distances, it reaches a maximum near R_c and then drops because most of the pairs have already recombined at smaller distances. For $R > 30R_c$ a power-law dependence was obtained,

$$\eta(R) \simeq A \left(\frac{R_c}{R} \right)^\beta, \quad (5)$$

$$P(R) \simeq \frac{A\beta}{R_c} \left(\frac{R_c}{R} \right)^{\beta+1}, \quad (6)$$

with $\beta = 1.16 \pm 0.01$ and $A = 3.0 \pm 0.1$.

Recently Baranovskii and Levin¹⁴ have computed $P(R)$ for the case when both the electron and the hole are mobile. In this case $P(R)$ depends on an additional parameter $\gamma = a_h/a_e$. Several curves $f_\gamma(R/R_c) \equiv R_c P_\gamma(R)$ for different values of γ are shown in Fig. 1, and we see that they become significantly broader and decay slower as γ increases. In the asymptotic expression

$$\eta_\gamma(R) \simeq A_\gamma \left(\frac{R_c}{R} \right)^{\beta_\gamma} \quad (7)$$

the index β_γ tends to 0.6 and A_γ tends to 2 as $\gamma \rightarrow 1$. The reason for such a change of the behavior is obvious: the motion of both carriers causes a larger separation of the pair and the diffusion competes better with the recombination. We note that the decay of the functions f_γ in Fig. 1 is very slow and that a significant contribution to their normalization comes from the unshown region $R > 5R_c$.

Shklovskii, Fritzsche, and Baranovskii⁸ suggested that in the limit of small generation rates most of the carriers recombine geminately and one can use $P(R)$ to describe the distribution of the logarithms of the recombination times $F(\ln t)$ which can be measured by TRS and FRS. This idea is based on Eq. (2), which relates the average recombination time ν_r^{-1} for a given configuration of states with the distance of the recombination R . Taking into account that $P(R)$ changes slowly on the length scale of a one obtains that the distribution of $\ln t$ should be the same as the distribution of $\ln \nu_r^{-1}$, i.e.,

$$\rho(R(t)) \simeq P(R(t)), \quad (8)$$

where $\rho(R(t)) \equiv (2/a_e)F(\ln t)$ and

$$R(t) \equiv \frac{1}{2}a_e \ln \left(\frac{t}{\tau_0} \right). \quad (9)$$

For convenience, we will use the distribution $\rho(R(t))$ instead of $F(\ln t)$ in what follows. Equation (8) is valid only for $G \rightarrow 0$ when all the pairs recombine geminately. Actually at any finite G some carriers that survive the geminate recombination recombine with nongeminate carriers. These distant-pair recombination processes are much slower than the geminate ones and the average lifetime τ is determined by them.

Now we would like to discuss the effect of distant-pair recombination on the function $\rho(R(t))$. To this end we first discuss the case where all the electrons and holes are created at random uncorrelated positions. This is the situation when the photon energies are larger than the mobility gap and the geminate carriers are well separated from each other after cooling down in the conduction and valence bands. Let us assume for simplicity that the carriers trapped in the tails are immobile and can only

recombine with each other. The same model was considered by Dunstan,¹⁵ but our results differ from his because he averaged the coefficients in his equations [see, e.g., Eqs. (4) and (5) in Ref. 15] rather than averaging the solution.

Suppose that at a given generation rate G the steady-state concentration of electrons and holes is n . The average lifetime of carriers is therefore

$$\tau = \frac{n}{G}. \quad (10)$$

There are two possibilities for any new electron arriving to the system. It can either recombine with an existing hole or, if the distance to the nearest existing hole is large such that $\nu_r^{-1} \gg \tau$, it will wait until a new hole arrives and will recombine with it. The survival probability of an electron at time t (i.e., the probability that it has not recombined during the time t) is a product of the probabilities that it did not recombine in either of these ways

$$w(t) = w_1(t)w_2(t). \quad (11)$$

If $t \gg \tau_0$ [i.e., $R(t) \gg a_e$], then any hole which is closer than $R(t)$ to the electron will recombine with it by the time t and therefore

$$w_1(t) = \exp \left[-\frac{4\pi}{3} [R(t)]^3 n \right] \quad (12)$$

is the probability that there are no holes, which already existed when the electron arrived, in a sphere with a radius $R(t)$ around the electron and

$$w_2(t) = \exp \left[-\frac{4\pi}{3} [R(t)]^3 G t \right] \quad (13)$$

is the probability that no new hole arrives into this sphere.

The mean lifetime τ is determined by $w(t)$:

$$\tau = \int_0^\infty t \left[-\frac{dw}{dt} \right] dt, \quad (14)$$

which after integrating by parts is

$$\tau = \int_0^\infty w(t) dt = \int_0^\infty \exp \left[-\frac{4\pi}{3} [R(t)]^3 (n + Gt) \right] dt. \quad (15)$$

$R(t)$ is a slow logarithmic function and therefore we can substitute $R(\tau)$ for $R(t)$ in Eq. (15) to obtain

$$\tau = \exp \left[-\frac{4\pi}{3} R_0^3 n \right] \frac{3}{4\pi R_0^3 G}, \quad (16)$$

where

$$R_0 \equiv R(\tau) = \frac{a_e}{2} \ln \left[\frac{\tau}{\tau_0} \right]. \quad (17)$$

Solving (10) and (16) we obtain

$$R_0 = \alpha n^{-1/3} \quad (18)$$

with $\alpha = \sqrt[3]{3z/4\pi} \approx 0.513$, where $z \approx 0.567$ is the root of the equation $\exp(-z) = z$. To find n for a given G we eliminate R_0 from Eqs. (18) and (17), which gives

$$\tau = \tau_0 \exp \left[\frac{2\alpha n^{-1/3}}{a_e} \right], \quad (19)$$

$$G = \frac{n}{\tau_0} \exp \left[\frac{-2\alpha n^{-1/3}}{a_e} \right], \quad (20)$$

and

$$\rho_d(R(t)) \equiv -dw/dR(t) = 4\pi R^2 n \left[1 + \left[1 + \frac{2R}{3a_e} \right] \exp[2(R - R_0)/a_e] \right] \exp \left[\frac{-4\pi}{3} R^3 n \{ 1 + \exp[2(R - R_0)/a_e] \} \right], \quad (23)$$

where R_0 and n are related by Eq. (18). We plot this distribution density in Fig. 2. For $R < R_0$, $\rho_d(R)$ coincides with the nearest-neighbor distribution and grows as R^2 while at $R \gtrsim R_0$ it decreases extremely rapidly with a decay length a_e . Therefore $\rho_d(R)$ has a sharp maximum at $R \sim R_0$. We also show in Fig. 2 the FRS distribution density $S(R)$ obtained from the TRS one as described in Appendix A.

We view the theory given above as a first approximation to the problem. We assumed that the holes are randomly distributed and that they do not recombine with any other electron in the time interval $(0, t)$. In spite of these approximations we will see that the computer-simulation results are in fair agreement with this theory.

Let us return now to the case where the electron and

$$n = \left[\frac{2\alpha}{a_e L} \right]^3, \quad (21)$$

where L is the solution of the equation

$$L = -\ln \left[G \tau_0 \left[\frac{\alpha_e L}{2\alpha} \right]^3 \right]. \quad (22)$$

For a typical experimental value $G = 10^{20} \text{ cm}^{-3} \text{ s}^{-1}$ and for $a_e = 1 \text{ nm}$, $\tau_0 = 10^{-8} \text{ s}$, Eq. (22) gives $L \approx 13$. The distribution density of $R(t)$ is

the hole are created in nearby states and spread out by downward hopping. Obviously most of the pairs that have reached a distance larger than R_0 will not recombine geminately and can be considered as created independently. Thus all the carriers can be divided in two parts: a fraction $1 - \eta(R_0)$ which recombines geminately and a fraction $\eta(R_0)$ which participates in distant-pair recombination. Therefore the function $\rho(R)$ is, roughly speaking, a superposition of $P(R)$ truncated at $R \approx R_0$ and $\rho_d(R)$ for distant-pair recombination with an effective generation rate $G\eta(R_0)$. One can say that all the tail of $P(R)$ for $R > R_0$ is converted to the distant-pair $\rho_d(R)$ with the normalization being conserved.¹¹ This modification of $\rho(R)$ is shown schematically in Fig. 3(a) for the case of very small G when R_0 is significantly

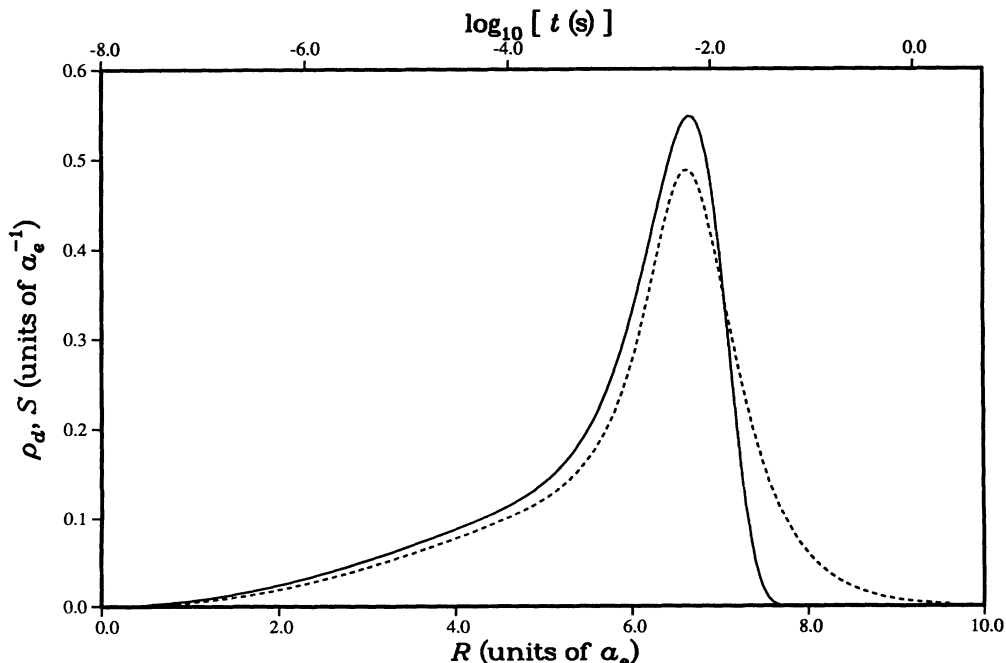


FIG. 2. The distributions of logarithms of lifetimes for the distant pair recombination obtained by the analytical theory described in Sec. II. The functions $\rho_d(R)$ and $S(R)$ are shown by a full line and dashed line, respectively.

larger than R_c . In Fig. 3(b) we show the case where R_0 and R_c are closer, distant-pair recombination dominates, and there is only one peak of $\rho_d(R)$.

To see how strongly the distant-pair recombination can affect $\rho(R)$ in *a*-Si:H let us estimate R_0 . We will see below that $\eta(R_0)$ is close to unity and therefore we can use Eqs. (22), (21), and (18) to find L and R_0 . For $a_e = 1$ nm, $\tau_0 = 10^{-8}$ s, and for a typical range of generation rates $10^{17} < G < 10^{22}$ cm $^{-3}$ s $^{-1}$ the quantity L changes from 18.9 to 9.5. This gives R_0 in the range $0.9R_c < R_0 < 2R_c$. Now we can use $P(R)$ to estimate the fraction of carriers which recombines geminately. For a reasonable choice $\gamma \equiv a_h/a_e = 0.7$ one gets values between 8% and 20% for the geminate fraction. Such a small fraction even at $R_0 = 2R_c$ is a consequence of the peculiar shape of $P(R)$, which has a very long and slowly decaying tail. Thus most of the carriers recombine non-geminately and the typical situation in *a*-Si:H should be described by Fig. 3(b). The computer simulation presented in the next section confirms these qualitative arguments.

III. THE COMPUTER SIMULATION

To study recombination and transport phenomena in amorphous semiconductors quantitatively we performed

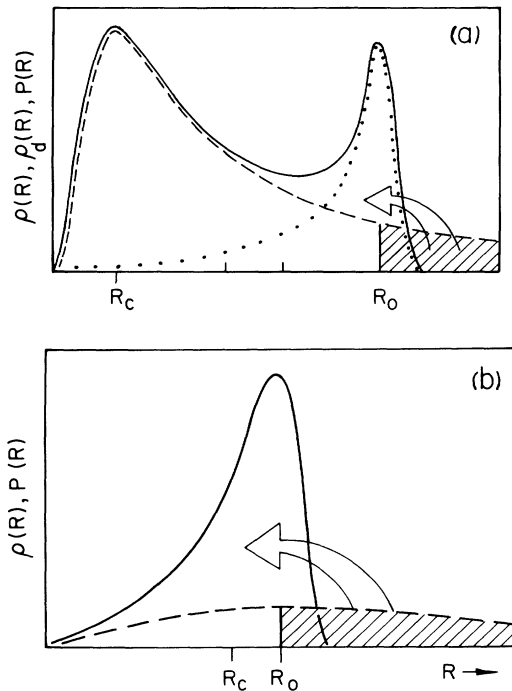


FIG. 3. The modification of $\rho(R)$ (full line) due to distant pair recombination (a) for small values of G and (b) for large values of G . The geminate recombination function $P(R)$ is shown by a dashed line and the distant pair on $\rho_d(R)$ by a dotted line. At $R > R_0$ [defined by Eq. (17)], $P(R)$ is truncated and the shaded tail is converted to the distant-pair recombination function.

a computer simulation, which we now describe. The idea was to generate localized electron and hole states with random coordinates and energies and to monitor the motion of carriers hopping between them. Three different processes are taken into account: (i) generation of new electron-hole pairs by a Poisson process with a constant rate G , (ii) hops of carriers from an occupied localized state to an empty one, and (iii) recombination between carriers of opposite types.

We use a cube with a side $B \gg a_e, a_h$ and randomly generate in it electron and hole states with concentrations N . The energies of these states are randomly distributed according to the density of states

$$g(\epsilon) = \frac{N}{\epsilon_0} \exp\left[-\frac{\epsilon}{\epsilon_0}\right] \quad (24)$$

with different characteristic tail widths (ϵ_{0h} or ϵ_{0e}) for the different types of carriers. Carrier energies are measured from the mobility edges into the mobility gap (downward for electrons and upward for holes). In *a*-Si:H the states in the mobility gap are neutral when empty and charged when occupied. The Coulomb interaction between carriers is neglected in our simulation.

The hopping rates from each site to sites situated deeper in energy are given by Eq. (1) for electrons and a similar expression for holes and decrease exponentially with the distance. Therefore we calculate the hopping rates only to the Q nearest neighbors of every site (assuming periodic boundary conditions) and neglect hopping to farther sites. The value of Q was varied in the range from 3 to 10 and we have checked that our results are independent of it.

Let us consider now the rates of the possible events in the system. For each carrier i currently situated on site l the hopping rate is

$$\gamma_i = \sum_k v_d(r_{lk})(1 - n_k), \quad (25)$$

where k runs over the Q neighbors of site l , r_{lk} are their distances from this site, and n_k is the occupation number of site k : $n_k = 1$ if the site is occupied and 0 if it is empty. The recombination rates for each pair are given by Eq. (2) and the total generation rate in the cube is GB^3 . When a new pair is generated we place one of its carriers on a random site and the other on the nearest site of the opposite type (if we investigate illumination with a photon energy close to the mobility gap) or on a random site of the opposite type (if we investigate illumination with a photon energy significantly larger than the mobility gap). These rates completely determine the behavior of the system and we use standard Monte Carlo techniques to monitor it.

We start from an empty system where only generation events are possible and let it evolve until the frequency of recombination events reaches that of generation ones. From here on the concentration of carriers fluctuates around a constant value and we assume this to be the steady state of the system. In the steady state we accumulate information about every recombination event: the lifetimes of the recombining carriers, their energies, and

the sum of these energies, which is the redshift of the emitted photon with respect to the gap. All these data are collected separately for geminate and nongeminate recombination events.

After the simulation is finished we use these data to calculate the mean lifetime τ , the mean concentration $G\tau$, and the fraction of geminate recombinations. We also obtain the probability densities $\rho_g(R(t))$ and $\rho_d(R(t))$ for geminate and distant-pair recombinations, respectively, the total probability density

$$\rho(R(t)) = \rho_g(R(t)) + \rho_d(R(t)), \quad (26)$$

and the spectrum of the emitted light. In order to obtain the FRS spectrum $S(R(t))$ we convolute $\rho(R(t))$ with the kernel described in Appendix A.

For the simulation we use a cube with $2NB^3 = 5 \times 10^5$ localized states. The number of states has to be so large because we want the number of steady-state electrons to be significantly larger than unity even at the lowest generation rates. The number of steady-state pairs varied from 40 to 400 in the range of generation rates presented in Fig. 4.

One simulation took 15 CPU minutes on a Cray-2 supercomputer. During this time there were approximately 10^5 generation and recombination events. Thus the time of the simulation was of the order of 10^3 lifetimes. This time was long enough to make the uncertainty in the average number of carriers less than 1. We have checked that for arrays of the size that we used the deviations between different realizations of the system were small. We therefore present below results for a single realization and do not use any averaging over different realizations.

IV. PHOTOLUMINESCENCE: SIMULATION RESULTS AND COMPARISON WITH EXPERIMENT

The complete set of dimensionless parameters in our problem is a_h/a_e , $G a_e^3/\nu_0$, $\nu_0\tau_0$, $\epsilon_{0h}/\epsilon_{0e}$, and $N a_e^3$. Most of our simulations were done using the following values: $a_h/a_e = 0.7$, $\nu_0\tau_0 = 10^4$, $\epsilon_{0h}/\epsilon_{0e} = 1.67$, and $N a_e^3 = 0.03$. Wherever it is possible we present our results both in dimensionless and in physical units. To compare our results with experiments on *a*-Si:H we use the following values of the parameters: $N = 3 \times 10^{19} \text{ cm}^{-3}$, $a_e = 1 \text{ nm}$, $a_h = 0.7 \text{ nm}$, $\nu_0 = 10^{12} \text{ s}^{-1}$, $\tau_0 = 10^{-8} \text{ s}$, $\epsilon_{0e} = 24 \text{ meV}$, and $\epsilon_{0h} = 40 \text{ meV}$. The exact values of these parameters are not known yet and one can consider the numbers given above as an illustration. Most of the results described below were obtained for the case when the carriers were generated on nearby sites.

The variations of the concentration of carriers $n = G\tau$ and the mean lifetime τ with G are shown in Fig. 4. We also show in the same plot the theoretical curves obtained using Eq. (20) with $\alpha = 0.513$, derived in Sec. II, and the experimental light-induced electron-spin-resonance data obtained by Boulitrop and Dunstan,¹⁶ and one can see that the results of our theory are in good agreement with the simulation results and with the experiment. The dependencies $n(G)$ and $\tau(G)$ can be fitted by a power law and we obtain $n \propto G^{0.16}$ and $\tau \propto G^{-0.84}$.¹⁷ The good agreement with the expressions derived for distant-pair recombination already shows that the distant-pair recombination dominates for these values of G . Indeed, the fraction of geminate recombinations is lower than 20% for all the values of G we have studied.

The good agreement of the theory for distant-pair recombination presented in Sec. II with the simulation re-

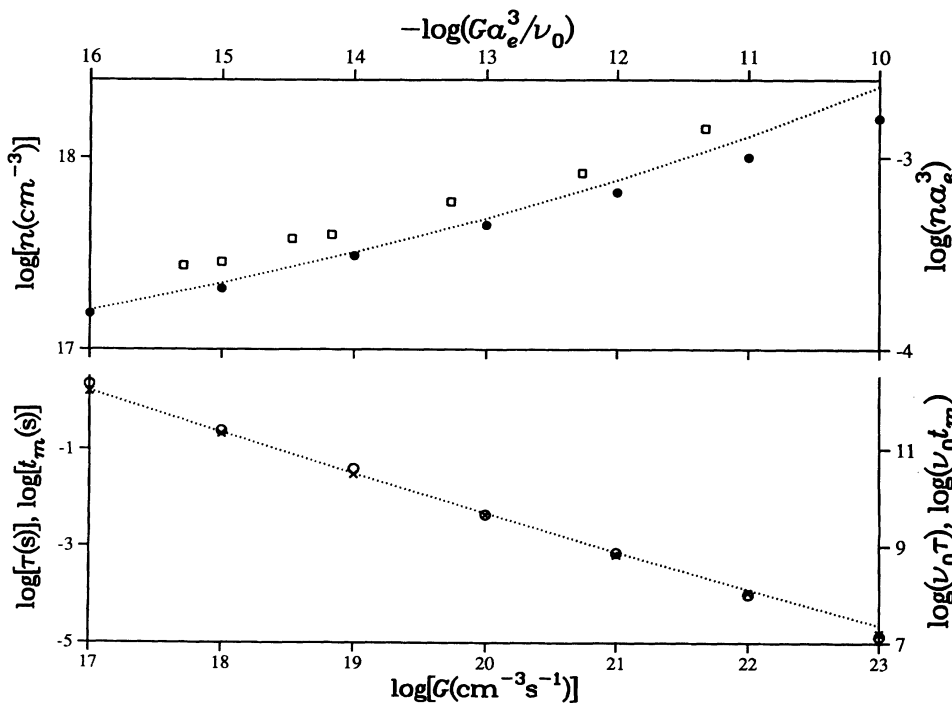


FIG. 4. Simulation results for the variations of the concentration of carriers n (full circles), the mean lifetime τ (open circles), and the time t_m corresponding to the peak of $\rho(R)$ (crosses) with the generation rate G . The dotted lines are the curves obtained by the theory derived in Sec. II, and the open squares are the experimental results obtained by Boulitrop and Dunstan (Ref. 16) (all the logarithms of the axis labels are in base 10).

sults and with the experiment deserves some further discussion. In our derivation we made two assumptions: (i) We assumed that carriers are trapped in localized states after they are generated and can participate only in recombination processes, and (ii) we assumed a uniform distribution of carriers in space. It was shown by Baranovskii, Ivchenko, and Shklovskii¹⁸ that the first assumption actually leads to some clustering of carriers of the same type resulting in a larger value of α ($\alpha=0.63$ in their simulation). We believe that the good agreement that we obtained using $\alpha=0.513$ is due to the fact that the hopping of carriers, which is taken into account in the simulation, reduces the effect of clustering and thus decreases the value of α . We verified this point by repeating our simulation for a case of static carriers (by turning off the hopping) and we indeed obtained $\alpha=0.625$ in this case. A theoretical treatment of PL taking into account the diffusion of carriers was recently published by the Leningrad group.¹⁹

We can get more information about the competition between geminate and distant-pair recombination from the distribution $\rho(R(t))$ for the logarithms of lifetimes. In Fig. 5 we show TRS functions $\rho(R(t))$ for three different values of the parameter Ga_e^3/ν_0 : 10^{-10} , 10^{-13} , and 10^{-16} . (For *a*-Si:H these values correspond to $G=10^{23}$, 10^{20} , and 10^{17} $\text{cm}^{-3}\text{s}^{-1}$.) We see that each curve has quite a narrow peak, which moves to shorter lifetimes with increasing G . The position of the peak t_m as a function of G is shown in Fig. 4 and one can see that it coincides exactly with the mean lifetime of carriers in the system (t_m is the time corresponding to the maximum of the density of the logarithm lifetime distribution). As

we have seen in Sec. II this is an important signature of the distant-pair recombination. The monotonic shift of the peak position according to $t_m \propto G^{-s}$ with $s=0.84$ is in qualitative agreement with the experimental data for the values $G > 10^{20}$ $\text{cm}^{-3}\text{s}^{-1}$.⁴ For $G < 10^{20}$ $\text{cm}^{-3}\text{s}^{-1}$ a slowing down or saturation of the motion of the peak position was reported.^{6,20} We do not see any change in the behavior of the peak position in our simulation. This probably means that some other physics should be taken into account to describe the observed phenomenon. To see whether nonradiative recombination, which we have neglected in our simulation, is involved, the dependence of the quantum efficiency on G should be studied experimentally. As for the width of the TRS peak at half height, we see in Fig. 5 that it is about two decades in lifetime and does not depend on G . This result agrees with the theory given in Sec. II and with the experimental data.⁴

More detailed information about $\rho(R(t))$ is presented in Fig. 6 for the value $Ga_e^3/\nu_0=10^{-13}$. In this case the fraction of carriers recombining geminately is 13%. In addition to the total distribution $\rho(R(t))$ we plot here $\rho_g(R(t))$ [see (26)] and also $P(R)$ for $\gamma=0.7$. One can see that ρ_g follows $P(R)$ up to values $R(t) \simeq 4a_e$. Since most of the latest measurements use the FRS technique we also show the FRS spectrum $S(R(t))$ obtained from our simulation using Eq. (A6). The FRS spectrum has a peak at the same position and with approximately the same width but decays more slowly for large times and has a more symmetric shape.

The fraction of carriers recombining geminately varies almost linearly with $\log_{10}G$ from 8% for $G=10^{-10}\nu_0a_e^{-3}$

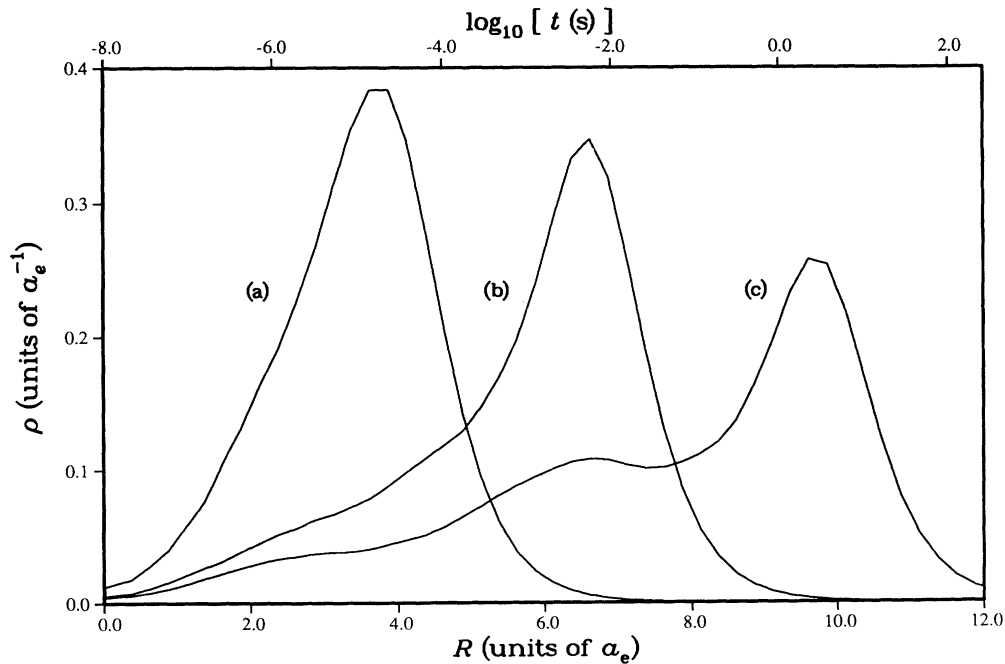


FIG. 5. The time-resolved spectroscopy functions $\rho(R(t))$ for three different values of the parameter Ga_e^3/ν_0 : (a) 10^{-10} , (b) 10^{-13} , and (c) 10^{-16} .

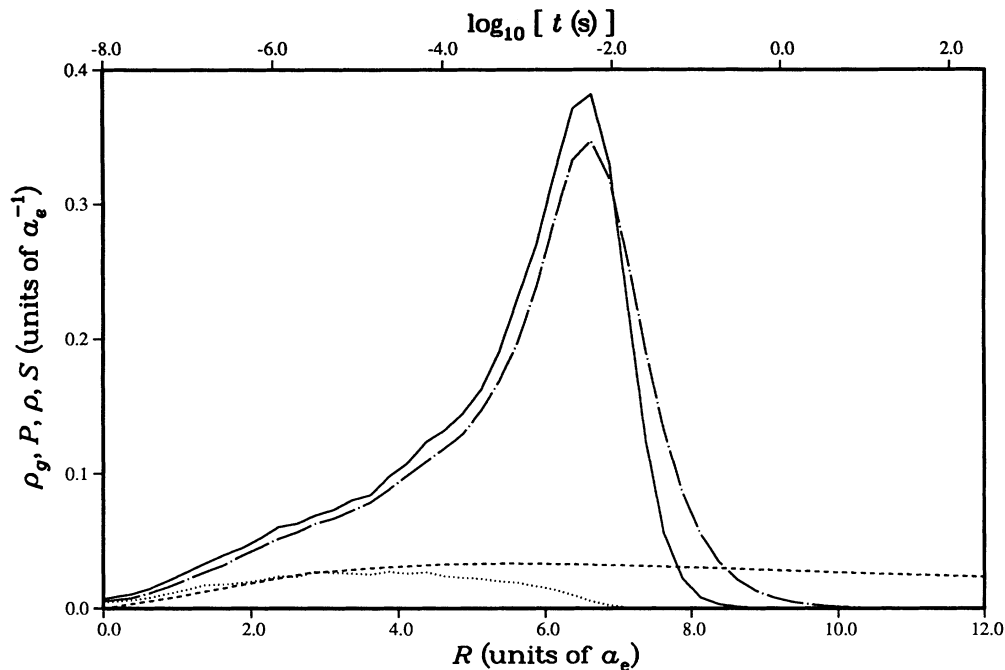


FIG. 6. $\rho(R(t))$ (full line), $\rho_g(R(t))$ (dotted line), and $S(R(t))$ (dashed-dotted line) as obtained by the computer simulation for the value $G a_e^3 / \nu_0 = 10^{-13}$. We also plot here the function $P(R)$ for $\gamma = 0.7$ (dashed line), and one can see that ρ_g follows $P(R)$ up to values $R(t) \approx 4a_e$.

to 19% for $G = 10^{-16} \nu_0 a_e^{-3}$. Thus we see that for typical generation rates in a -Si:H the geminate recombination plays a minor role. We have verified that decreasing G far below $10^{-16} \nu_0 a_e^{-3}$ ($10^{17} \text{ cm}^{-3} \text{ s}^{-1}$) increases the part

of geminate recombination and we can get a spectrum like the one shown in Fig. 3(a). Moreover, at extremely small $G = 10^{-80} \nu_0 a_e^{-3}$ we obtain $\rho(R) = P(R)$ for all $R < B$ and there are no distant-pair recombinations at all.

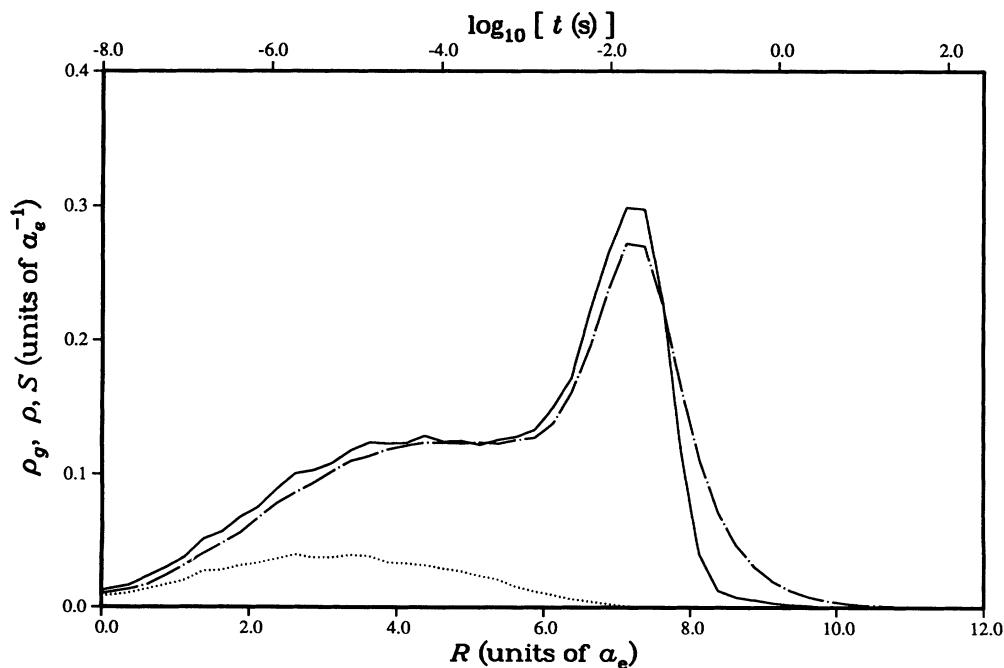


FIG. 7. $\rho(R(t))$ (full line), $\rho_g(R(t))$ (dotted line), and $S(R(t))$ (dashed-dotted line) obtained by the simulation for $\gamma \equiv a_n / a_e = 0$ and $G = 10^{-13} \nu_0 a_e^{-3}$.

Another way to increase the role of the geminate recombination is to consider a smaller value of $\gamma = a_h/a_e$, since in Fig. 1 we see that geminate recombination at small distances grows with decreasing γ . In Fig. 7 we show $\rho(R(T))$ obtained for $\gamma=0$ and $G=10^{-13}\nu_0 a_e^{-3}$. We see that the left shoulder of $\rho(R)$ grows, in comparison with the one in Fig. 6, but the position and the width of the peak remain unchanged. The fraction of geminate

recombinations increases from 13% for $\gamma=0.7$ to 17.5% for $\gamma=0$ as could be expected from Fig. 1.

More interesting changes in the TRS and FRS spectra take place when the parameter $\nu_0\tau_0$ decreases. As mentioned by Baranovskii *et al.*,⁹ the frequency of downward hopping can be significantly diminished by a polaron effect, while τ_0 stays unaffected. In Fig. 8 we present the results of our simulation for $\nu_0=10^9 \text{ s}^{-1}$ and

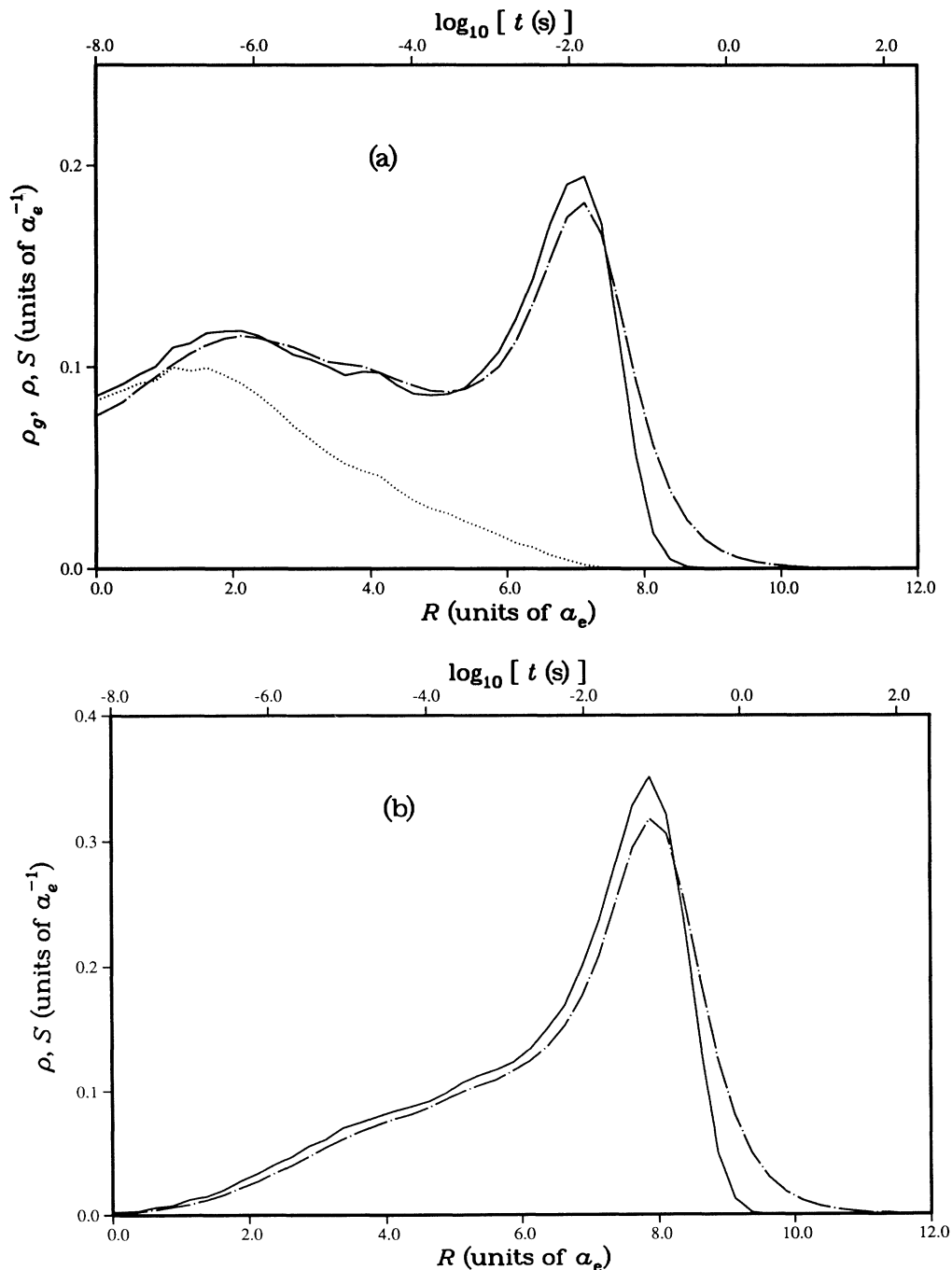


FIG. 8. (a) The distribution densities $\rho(R(t))$ (full line), $\rho_g(R(t))$ (dotted line), and $S(R(t))$ (chain-dotted line) for a diffusion rate $\nu_0=10^9 \text{ s}^{-1}$, a recombination rate $\tau_0=10^{-8} \text{ s}$, and for a generation rates $G=10^{20} \text{ cm}^{-3} \text{ s}^{-1}$. (b) The same as (a) but with carriers generated at random sites.

$\tau_0 = 10^{-8}$ s. According to Eq. (3), R_c decreases with ν_0 and the geminate peak which is situated at R_c should move to smaller R and split from the nongeminate one. In order to keep the intensity of light at a typical experimental value, we choose first $G = 10^{20} \text{ cm}^{-3} \text{ s}^{-1}$ (the same as that in Fig. 6). Indeed we see in Fig. 8(a) a two-peak structure similar to the schematic plot in Fig. 3(a). At smaller values of G this two-hump structure is even more pronounced. On the other hand, when the pairs are generated at random points (i.e., when the photon energies are above the mobility gap), for the same values of the parameters, the left peak of $\rho(R)$ disappears [see Fig. 8(b)]. At the same time when $\nu_0 = 10^{12} \text{ s}^{-1}$ random generation of carriers leads only to minor changes of the spectra at small values of R (compare Fig. 9 and Fig. 6). This demonstrates again that geminate recombination plays only a minor role in *a*-Si:H.

In experiments with materials that have small hopping rates ν_0 one can expect a crossover from a one-peak structure to a two-peak one when the wavelength of the illumination increases. At $h\nu > E_g$ the pairs separate during the cooling down in the delocalized states and only the distant-pair recombination peak can be observed, while at $h\nu < E_g$ both peaks should be seen. Such a crossover has been observed in the As_2S_3 glass,²¹ which can be a good candidate for a strong polaron effect, but the original interpretation was done totally in terms of the geminate picture. Our attempts to interpret the data in light of the present work failed because our estimates of the carrier concentration based on the data given in²¹ result in too small values to expect any distant-pair recombination.

Let us now compare the results of our simulation for random generation of carriers with the theoretical derivation of the distant-pair recombination probability density $\rho_d(R)$ presented in Sec. II. The results are shown in Figs. 2 and 9 and one can see that they are quite close and differ mostly in the right tail, which is less steep for the results of the simulation. The reason for this difference is that in the process of downward hopping the flux of additional carriers to sites from which they recombine varies due to random fluctuations in spatial configurations. These fluctuations, which are taken into account in the simulation, smear out the steep tail of $\rho(R)$. On the other hand, in the theoretical derivation there was no downward hopping of carriers and we assumed that the flux to each site is constant and is determined only by the generation rate G .

To end the part dealing with TRS and FRS spectra we now briefly discuss the role of the Coulomb interaction in *a*-Si:H. It was argued,⁸ for the geminate recombination function $P(R)$, that the Coulomb interaction cannot compete with the characteristic energy of "disorder" ϵ_0 at distances $R > R_c$ and will not change the shape of $P(R)$ at these distances (see also Ref. 6). Our recent estimates show that at $R < R_c$ the Coulomb interaction should be important and can result in a significant increase of $P(R)$. This "excitonic" effect will show up at small R values in TRS and FRS spectra but will not affect other parts of the spectra. The Coulomb effects will be discussed in a separate publication.

Let us return to *a*-Si:H and discuss our results for the energy spectrum of luminescence shown in Fig. 10. The luminescence intensity is presented as a function of

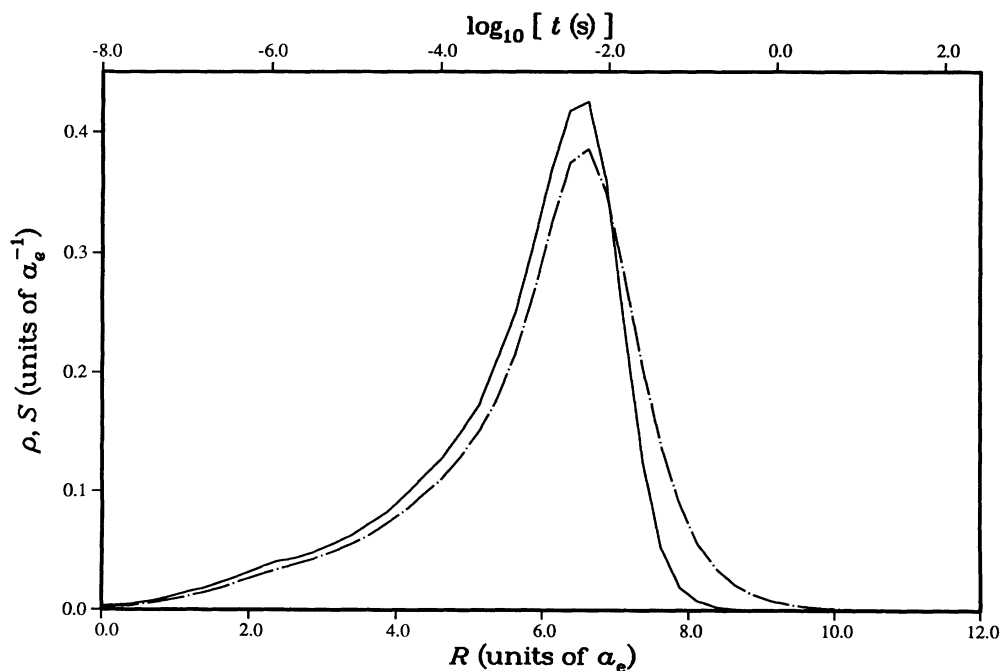


FIG. 9. $\rho(R(t))$ (full line) and $S(R(t))$ (dashed-dotted line) for the same parameters as in Fig. 6 but with carriers generated at random sites. We see that while the geminate recombination is completely suppressed, there are only small changes in ρ and S .

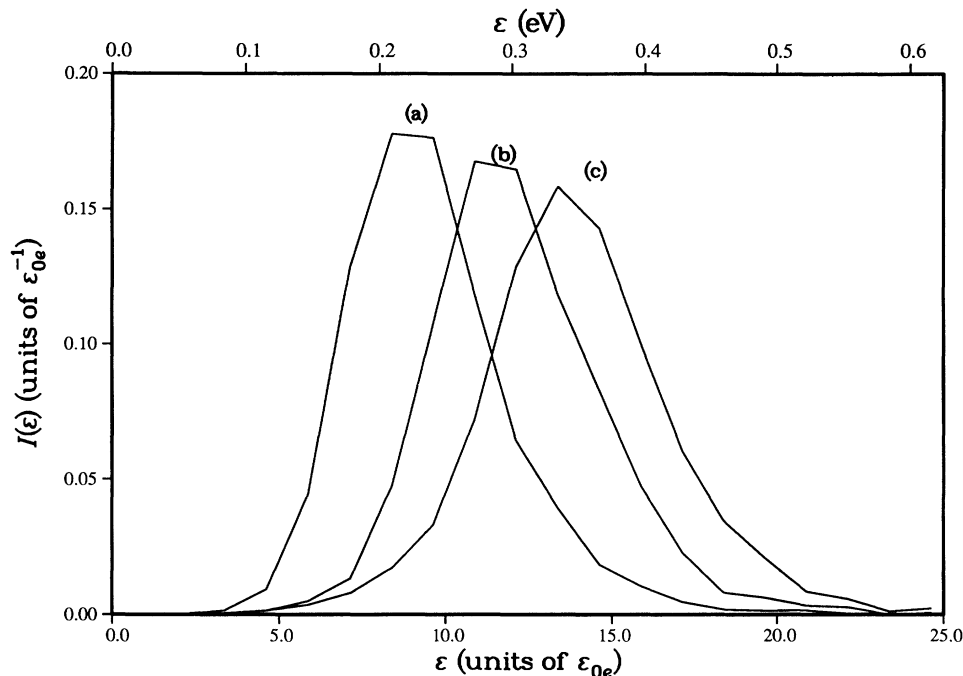


FIG. 10. The spectra $I(\epsilon)$ for three different values of the parameter $G a_e^3 / \nu_0$: (a) 10^{-10} , (b) 10^{-13} , and (c) 10^{-16} .

$E_g - h\nu$ in units of ϵ_{0e} for different values of G . We see that a typical shift of the luminescence peak $E_g - h\nu_{\max} \approx 13\epsilon_{0e} \approx 0.32$ eV, which is less than the 0.4-eV shift observed in the experiment. We have to mention, however, that this shift is the only quantity which depends on N and, generally speaking, on the behavior of the density of states near the mobility edges. If N increases from $3 \times 10^{19} \text{ cm}^{-3}$ to 10^{20} cm^{-3} one gets $E_g - h\nu_{\max} \approx 16\epsilon_{0e} \approx 0.4$ eV in agreement with the experiment. On the other hand, the width of the peak does not depend on N and G and equals $6\epsilon_{0e}$. This result is in agreement with the theory of Dunstan and Boulitrop⁶ but is almost a factor 2 less than the experimental value.⁵ This probably means that there are fluctuations of the mobility gap which can result from fluctuations in the hydrogen content. As for the position of the peak of the spectrum, we find that it has a blueshift with increasing generation rate G and that it is approximately equal to $0.85\epsilon_{0e}$ per decade of G . This shift is about twice as large as the experimental value reported by Tsang and Street.²²

V. CONCLUSIONS

We have studied the transition between geminate and distant-pair recombination with increasing generation rate in amorphous semiconductors. We found that in a -Si:H, where the prefactor of the hopping rate is believed to be four orders larger than that of the combination rate, the geminate recombinations contribute less than 20% to the total photoluminescence for typical experimental generation rates that are larger than $10^{17} \text{ cm}^{-3} \text{ s}^{-1}$. We obtained the shape and position of the photoluminescence peaks of TRS with a bias and FRS as a function of the generation rate. The width of the peaks is approximately

two decades in time or frequency in the whole range of generation rates, in good agreement with experimental results. We have shown that geminate recombination can become more important for materials with smaller hopping rates. In this case one can observe two separate peaks of TRS or FRS spectra, one due to geminate recombination and the other due to distant-pair recombination.

The photoluminescence results presented in this paper were obtained for a situation where the system undergoes small perturbations on the background of a steady-state concentration of photoexcited carriers. These conditions are obtained experimentally for TRS with a bias or for FRS. We now briefly discuss the case of TRS without a bias when a system in equilibrium is excited by a short single pulse of duration δt . The shape of the lifetime distribution of distant-pair recombinations for this case was derived by Dunstan²³ and is given by

$$\rho(R) = 4\pi R^2 G \delta t \left[1 + \frac{4\pi}{3} R^3 G \delta t \right]^{-2}. \quad (27)$$

This distribution has a peak at $R = R_1 / \sqrt[3]{2}$, where $(4\pi/3)R_1^3 G \delta t = 1$, and a width $1.1R_1$. This width is significantly larger than the width obtained in Sec. II for steady-state conditions (see also Fig. 2) and than any width obtained experimentally. This probably means that in realistic experimental conditions when the sample is excited by a sequence of pulses it is difficult to avoid accumulation of photocarriers. Due to these difficulties we did not study TRS without a bias in our computer simulation.²⁴

The computer simulation that we developed for the description of steady-state properties such as carrier con-

centration and photoluminescence at zero temperature can be applied to many other phenomena in amorphous semiconductors. We are currently planning to include an electric field in the simulation and to study both the linear and the non-Ohmic photoconductivity. These can be used to check existing theoretical predictions¹³ and can also be directly compared with experiment. The next step will be to study the effects of doping and finite temperature on transport phenomena in amorphous semiconductors and in particular to test theoretical predictions about the correspondence between the temperature and electric-field dependence of the conductivity.¹³

ACKNOWLEDGMENTS

We are grateful to S. Baranovskii, H. Fritzsche, W. Fuhs, J. Kakalios, I. Ruzin, and R. Street for stimulating discussions and careful reading of the manuscript. This work was supported by the National Science Foundation under Grant No. DMR-9020587 and by a grant from the Minnesota Supercomputer Institute.

APPENDIX A: THE RELATION BETWEEN TRS AND FRS

Throughout the paper we have discussed the photoluminescence of amorphous semiconductors in terms of both TRS (time-resolved spectroscopy) and FRS (frequency-resolved spectroscopy). In a TRS experiment the sample is excited by a δ -function light pulse and the distribution $p(t)$ of lifetimes of photocarriers is obtained from the luminescence detected at some time t_d after the pulse. An alternative experimental technique is the FRS in which the sample is excited by a continuous modulation with a frequency ω , $\sin\omega t$, and the detector is set at a phase shift of $-\pi/2$ (i.e., $-\cos\omega t$) to the excitation wave. In this appendix we derive the relation between the distribution $\rho(R(t))$ of logarithms of lifetimes

$$R(t) = \frac{a_e}{2} \ln \left[\frac{t}{\tau_0} \right], \quad (\text{A1})$$

which is obtained by TRS, and the signal intensity $S(R'(\omega))$

$$R'(\omega) = \frac{a_e}{2} \ln \left[\frac{1}{\omega\tau_0} \right], \quad (\text{A2})$$

which is obtained in a FRS experiment.

The output signal from the detector is

$$s(\omega) = -\frac{\omega}{2\pi} \int_0^{2\pi/\omega} I(t) \cos(\omega t) dt, \quad (\text{A3})$$

where $I(t)$ is the luminescence excited by the continuous modulation. If the distribution density of lifetimes of the photoexcited carriers is $p(t)$, then $I(t)$ is given by

$$I(t) = \int_{-\infty}^t p(t-t') \sin(\omega t') dt'. \quad (\text{A4})$$

Substituting Eq. (A4) in Eq. (A3) we obtain

$$s(\omega) = \frac{1}{2} \int_0^{\infty} p(t) \sin(\omega t) dt. \quad (\text{A5})$$

To obtain the relation between $\rho(R(t))$ and $S(R'(\omega))$ we substitute Eqs. (A1) and (A2) in Eq. (A5) using the identity $\rho(R)dR \equiv p(t)dt$. We also set the normalization of the transformation by the condition that it should transform a constant into itself. The final expression is given by

$$S(R') = \frac{4}{a_e \pi} \int_{-\infty}^{\infty} \sin \left[\exp \left(\frac{2(R-R')}{a_e} \right) \right] \rho(R) dR. \quad (\text{A6})$$

The kernel $(4/\pi a_e) \sin[\exp(x/a_e)]$ of the transformation tends to a δ function in the limit $a_e \rightarrow 0$ thus giving $S(R) = \rho(R)$ in this limit. For finite values of a_e the kernel strongly oscillates for positive values of x and decays exponentially for negative ones. Therefore the main contribution to the integral in Eq. (A6) comes from $R \simeq R'$ and, as we see in Figs. 2 and 5, the general shape of $\rho(R)$ is reproduced by $S(R)$. For $R > R_0$ the distribution $\rho(R)$ has a sharp decrease (see Sec. II) and the tail of $S(R)$ is broader than that of $\rho(R)$.

We note that Eq. A5 differs from the one which relates the distribution of *relaxation times* $\tilde{p}(\tau)$ to $s(\omega)$:

$$s(\omega) = \frac{1}{2} \int_0^{\infty} \tilde{p}(\tau) \frac{\omega\tau}{1+\omega^2\tau^2} d\tau. \quad (\text{A7})$$

The distribution of lifetimes $p(t)$ is given by

$$p(t) = \int_0^{\infty} \frac{\exp(-t/\tau)}{\tau} \tilde{p}(\tau) d\tau. \quad (\text{A8})$$

Substituting Eq. (A8) in Eq. (A5) one can easily get Eq. (A7).

¹M. Hoheisel, R. Carius, and W. Fuhs, J. Non-Cryst. Solids **59&60**, 457 (1983); **63**, 313 (1984).

²H. Vomvas and H. Fritzsche, J. Non-Cryst. Solids **97&98**, 823 (1987).

³T. M. Searle, M. Hopkinson, M. Edmeades, S. Kalem, I. G. Austin, and R. A. Gibson, *Disordered Semiconductors*, edited by M. A. Kastner, G. A. Thomas, and S. R. Ovshinsky (Plenum, New York, 1987).

⁴M. Bort, R. Carius, and W. Fuhs, in *Proceedings of the 13th International Conference on Amorphous and Liquid Semiconductors, Asheville*, edited by M. Paesler, S. G. Agarwal, and R. Zallen (North-Holland, Amsterdam, 1989).

⁵R. A. Street, Adv. Phys. **30**, 593 (1981).

⁶D. J. Dunstan and F. Boulitrop, Phys. Rev. B **30**, 5945 (1984).

⁷T. M. Searle, Philos. Mag. Lett. **61**, 251 (1990).

⁸B. I. Shklovskii, H. Fritzsche, and S. D. Baranovskii, Phys. Rev. Lett. **62**, 2989 (1989).

⁹S. D. Baranovskii, H. Fritzsche, E. I. Levin, I. M. Ruzin, and B. I. Shklovskii, Zh. Eksp. Teor. Fiz. **96**, 1369 (1989) [Sov. Phys. JETP **69**, 773 (1989)].

¹⁰S. P. Depinna and D. J. Dunstan, Philos. Mag. B **50**, 579 (1984).

¹¹E. I. Levin, S. Marianer, B. I. Shklovskii, and H. Fritzsche, J. Non-Cryst. Solids **137&138**, 559 (1991).

- ¹²M. Vaněček, J. Kočka, P. Demo, E. Sipek, and A. Triška, *J. Non-Cryst. Solids* **90**, 183 (1987).
- ¹³B. I. Shklovskii, E. I. Levin, H. Fritzsche, and S. D. Baranovskii, in *Transport, Correlations and Structural Defects*, edited by H. Fritzsche (World Scientific, Singapore, 1990), p. 161.
- ¹⁴S. D. Baranovskii and E. I. Levin (unpublished).
- ¹⁵D. J. Dunstan, *Philos. Mag. B* **52**, 111 (1985).
- ¹⁶F. Boulitrop and D. J. Dunstan, *Solid State Commun.* **44**, 841 (1982); *J. Non-Cryst. Solids* **77&78**, 663 (1985).
- ¹⁷It was suggested (S. D. Baranovskii and B. I. Shklovskii, *Fiz. Tekh. Poluprovodn.* **23**, 146 (1989) [*Sov. Phys. Semicond.* **23**, 88 (1989)]) that at high generation rates G when $n^{-1/3} < R_c$, the variation of n with G is of the form $n \propto \sqrt{G}$. We believe now that this result is incorrect. It was based on the assumption that typical hops by which carriers diffuse into close pairs of electron and hole states (which are responsible for most of the recombinations in this case) have a length of the order of $n^{-1/3}$. Actually at zero temperature, when only downward hopping is possible, carriers have to use much longer hops in order to travel the long distance to a close pair of states. Therefore the recombination will continue to be diffusion limited and the concentration will have a weak logarithmic dependence on G even in this range of large n .
- ¹⁸S. D. Baranovskii, E. L. Ivchenko, and B. I. Shklovskii, *Zh. Eksp. Teor. Fiz.* **92**, 2234 (1987) [*Sov. Phys. JETP* **65**, 1260 (1987)].
- ¹⁹A. G. Abdukadyrov, S. D. Baranovskii, and E. L. Ivchenko, *Fiz. Tekh. Poluprovodn.* **24**, 136 (1990) [*Sov. Phys. Semicond.* **24**, 82 (1990)].
- ²⁰R. Stachowitz, M. Bort, R. Carius, W. Fuhs, and S. Liedtke, *J. Non-Cryst. Solids* **137&138**, 551 (1991).
- ²¹G. S. Higashi and M. A. Kastner, *Philos. Mag. B* **47**, 83 (1983).
- ²²C. Tsang and R. A. Street, *Phys. Rev. B* **19**, 3027 (1979).
- ²³D. J. Dunstan, *Philos. Mag. B* **49**, 191 (1984).
- ²⁴In a series of papers (J. R. Eggert, *Phys. Rev. B* **29**, 6664 (1984); T. M. Searle and J. E. L. Bishop, *Philos. Mag. B* **53**, L9 (1986); M. Foygel, *Fiz. Tekh. Poluprovodn.* **21**, 1147 (1987) [*Sov. Phys. Semicond.* **21**, 699 (1987)]) it was shown that if electrons and holes are created randomly in space, $\rho(R)$ decays at long times even slower than in Eq. (27): [$\rho(R) \propto R^{-5/2}$]. In the case of low-frequency illumination, when pairs are spread by hopping, there are no fluctuations on scales larger than R_1 if $R_1 \geq R_c$. The pairs simply do not have enough time to spread to larger distances before they recombine. In this case Eq. (27) is valid. In other cases (for $R_1 \leq R_c$) the distribution of lifetimes is even broader and the contradiction with experiment that was mentioned above is even more severe.